

## Rolling quantum dice with a superconducting qubit

R. Barends,<sup>1</sup> J. Kelly,<sup>1</sup> A. Veitia,<sup>2</sup> A. Megrant,<sup>1</sup> A. G. Fowler,<sup>1,3</sup> B. Campbell,<sup>1</sup> Y. Chen,<sup>1</sup> Z. Chen,<sup>1</sup> B. Chiaro,<sup>1</sup> A. Dunsworth,<sup>1</sup> I.-C. Hoi,<sup>1</sup> E. Jeffrey,<sup>1</sup> C. Neill,<sup>1</sup> P. J. J. O'Malley,<sup>1</sup> J. Mutus,<sup>1</sup> C. Quintana,<sup>1</sup> P. Roushan,<sup>1</sup> D. Sank,<sup>1</sup> J. Wenner,<sup>1</sup> T. C. White,<sup>1</sup> A. N. Korotkov,<sup>2</sup> A. N. Cleland,<sup>1</sup> and John M. Martinis<sup>1</sup>

<sup>1</sup>Department of Physics, University of California, Santa Barbara, California 93106, USA

<sup>2</sup>Department of Electrical Engineering, University of California, Riverside, California 92521, USA

<sup>3</sup>Centre for Quantum Computation and Communication Technology, School of Physics, The University of Melbourne, Victoria 3010, Australia

(Received 15 July 2014; published 22 September 2014)

One of the key challenges in quantum information is coherently manipulating the quantum state. However, it is an outstanding question whether control can be realized with low error. Only gates from the Clifford group—containing  $\pi$ ,  $\pi/2$ , and Hadamard gates—have been characterized with high accuracy. Here, we show how the Platonic solids enable implementing and characterizing larger gate sets. We find that all gates can be implemented with low error. The results fundamentally imply arbitrary manipulation of the quantum state can be realized with high precision, providing practical possibilities for designing efficient quantum algorithms.

DOI: 10.1103/PhysRevA.90.030303

PACS number(s): 03.67.Lx, 03.65.Wj, 85.25.Cp

The Platonic solids have been studied since ancient times for their beauty and symmetry [1], and make excellent random number generators [2]. Here, we exploit their symmetry for quantum information. Quantum processing would benefit from having a large set of accurate gates to reduce gate count and error [3–5], yet it is an open question whether arbitrary gates can be implemented with low error—only the restricted group of Clifford gates [6,7] has been used with high precision [8–10]. We use the Platonic solids as a pathway and implement gate sets inspired by the tetrahedron, octahedron, and icosahedron, including gates never previously benchmarked. We achieve low error for all gates. These results illustrate the potential of using unitaries with a fine distribution, and suggest arbitrary rotations can be realized with high accuracy, opening new avenues for performing gates and designing algorithms efficiently.

Recently, major advances have been made in accurately implementing Clifford gates on a variety of platforms. Superconducting qubits, liquid NMR, and ion traps have shown single-qubit gate errors ranging from  $10^{-3}$  to  $10^{-6}$  [8–10], determined via Clifford-based randomized benchmarking (RB). Arbitrary rotations—for quantum chemistry and quantum simulation [3–5]—can then be approximated by sequences of Clifford and non-Clifford gates [6]. To minimize the accumulation of gate error when implementing these algorithms in present-day quantum processors, one would like to perform such rotations directly. However, high fidelity rotations outside of the Clifford group are yet to be demonstrated. Process verification of non-Clifford gates is a conundrum: Quantum process tomography can be used, but state preparation and measurement error can lead to significant systematic deviations, limiting precision. Clifford-based RB is insensitive to these errors, but unavailable for gates which fall outside of the Clifford group.

Here, we demonstrate the high fidelity implementation of non-Clifford gates, by using larger rotational groups. Our approach also opens the door to evaluating functions of higher order, and experimentally tests a core premise—that any unitary 2-design is sufficient—of randomized benchmarking, a technique that is becoming a keystone metric in quantum information. A different approach to estimating errors of non-Clifford gates was proposed in Ref. [11].

The groups of unitaries we use here are formed by the rotations that preserve the regular tetrahedron, octahedron, and icosahedron—Platonic solids—in the Bloch sphere representation (see Fig. 1). These are the rotational subgroups of the tetrahedral, octahedral, and icosahedral symmetry groups  $T_h$ ,  $O_h$ , and  $I_h$ . These rotations exchange faces, amounting to a quantum version of rolling dice (such dice are referred to as d4, d8, and d20), but now in Bloch space. The tetrahedral, octahedral, and icosahedral rotational groups have size (order) 12, 24, and 60, respectively. The axes are defined by the lines that intersect the origin, and a face center, vertex, or midpoint of an edge. The angles of rotation around these axes are, respectively, integer multiples of  $\{2\pi/3, 2\pi/3, \pi\}$  for the tetrahedral group,  $\{2\pi/3, 2\pi/4, \pi\}$  for the octahedral group, and  $\{2\pi/3, 2\pi/5, \pi\}$  for the icosahedral group. The tetrahedral rotations (orange axes in Fig. 1) are shared among all three groups, enabling comparison experiments. The octahedral rotations form the single-qubit Clifford group. The icosahedral rotations form the most dense group—the icosahedron is the largest of the Platonic solids—allowing for fine unitary control.

For implementing gates from these groups we decompose them into rotations around the  $X$ ,  $Y$ , and  $Z$  axes. The tetra- and octahedral groups can be implemented using only  $\pi/2$  and  $\pi$  rotations [12]. The icosahedral group requires the rotation

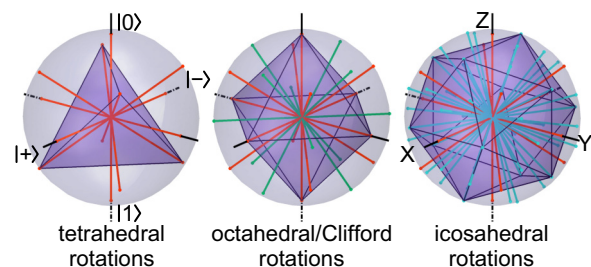


FIG. 1. (Color online) The Platonic solids and their rotational groups. The axes of rotation are of the tetra-, octa-, and icosahedral rotational group; the respective Platonic solids are superimposed. The axes are defined by lines intersecting the origin, and a vertex, face center, or midpoint of an edge. The tetrahedral rotational group (orange) is shared among all groups.

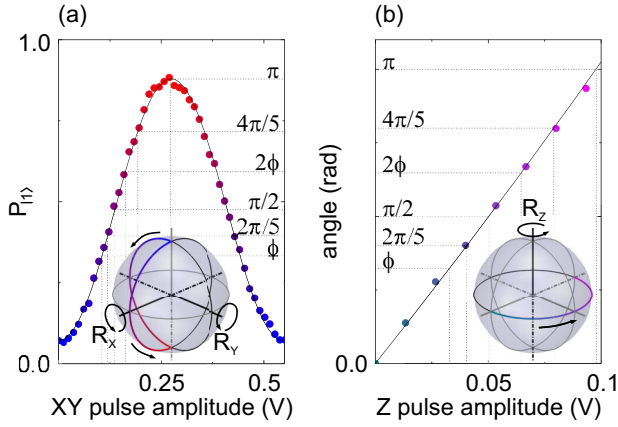


FIG. 2. (Color online) Calibrating the angles of rotation. (a) The excited state probability versus  $X$  and  $Y$  pulse voltage amplitude on the control board. The amplitudes for the required phases of rotations around the  $X$  and  $Y$  axes are indicated with dotted lines. The data follow a  $\sin^2$  dependence (solid line) on the pulse amplitude, as expected. Data are not corrected for measurement fidelity. (b) The phase of the quantum state as a function of  $Z$  pulse voltage amplitude, measured using quantum state tomography. Solid line is a fit to the data. For brevity, only the positive angles are shown. Here  $\tan \phi = (1 + \sqrt{5})/2$ . Insets show the trajectories on the Bloch sphere for the  $X$ -,  $Y$ -, and  $Z$ -axis rotations.

angles  $\{\phi, 2\pi/5, \pi/2, 2\phi, 4\pi/5, \pi\}$ , with  $\phi$  an irrational angle from  $\tan \phi = (1 + \sqrt{5})/2$  the golden ratio. The decomposition into physical gates is shown in the Supplemental Material [13]. The average number of physical gates per tetra-, octa-, or icosahedral rotation is  $1\frac{3}{4}$ ,  $1\frac{7}{8}$ , and  $4\frac{4}{15}$ , respectively. This decomposition requires a minimal number of used angles and only one irrational angle.

The rotations are implemented in our superconducting quantum system, the Xmon transmon qubit [14]. This qubit combines full, direct axial control with a high level of coherence. Details of the device used in this experiment can be found in Ref. [8]. Rotations around the  $X$  and  $Y$  axes are achieved by applying microwave pulses. Rotations around the  $Z$  axis can be directly performed by detuning the qubit frequency, or by combining  $X$  and  $Y$  rotations. All control pulses have cosine envelopes, generated by fast (1 Gsample/s) digital-to-analog converter boards. For  $XY$  control we generate both the in-phase and quadrature component and upconvert it to the qubit frequency using quadrature mixing (see Supplemental Material [13] and Refs. [8,15] for more detail). For calibrating the pulse amplitudes we use the measured probability for  $X$  and  $Y$  rotations, and for  $Z$  rotations the phase as determined using quantum state tomography (Fig. 2). We minimize leakage to energy levels above the computational subspace by applying a quadrature correction [16,17]. Subsequently, fine-tuning of the parameters is done through optimized randomized benchmarking for immediate tune-up (ORBIT) [15], reducing gate errors by approximately  $10^{-4}$  [18]. The generators of the tetrahedral and octahedral groups are fully parametrized by a total of three parameters, and the generators of the icosahedral group by a total of 14 variables (see Supplemental Material [13]).

We test the gates using randomized benchmarking [8–10,12,19]. In essence, randomized benchmarking is equivalent to randomly rolling the die in Bloch space  $m$  times followed by a final rotation that returns it to the starting position, and then measuring the probability of success. One would like to determine the gate error averaged over all possible input states. As the gate error depends quadratically on, for example, any amount of over- or under rotation, we do not need to evaluate a continuum of input states. The average of a polynomial function of order  $t$  over the surface of a sphere can be evaluated exactly using only a finite number of points; such a group of points is a spherical  $t$ -design. For the single-qubit case, unitary designs are the group of rotations that can generate spherical designs, mapping between the points [20]. Therefore, the rotational group used in randomized benchmarking needs to be a unitary 2-design [20–23]. Moreover, unitary 2-designs depolarize any error in the computational basis. For the single-qubit case, the rotational groups which preserve Platonic solids are the 2-designs [24]. There are only three unitary 2-designs as the cube shares the same group as the octahedron (the cube and the octahedron are duals), and the dodecahedron shares the same rotations as the icosahedron (the dodecahedron and the icosahedron are duals). We have thus tested all unitary 2-designs in Bloch space.

Randomized benchmarking with 2-designs is therefore a crucial test of coherent control. The decrease of the probability of success—the sequence fidelity—with increasing sequence length is used to quantify the gate fidelity. We start by measuring a reference curve, using sequences of  $m$  random rotations. The sequence fidelity follows  $Ap^m + B$ , with variables  $A$  and  $B$  absorbing measurement and initialization errors, and  $p_{\text{ref}}$  giving the average error per rotation:  $r_{\text{ref}} = (1 - p_{\text{ref}})/2$  [19]. We then interleave a specific gate with  $m$  random rotations; the difference with the reference is a direct measure of the gate error:  $r_{\text{gate}} = (1 - p_{\text{gate}}/p_{\text{ref}})/2$ ; the gate fidelity is  $F_{\text{gate}} = 1 - r_{\text{gate}}$  [25]. At each  $m$ , the data is averaged over  $k = 50$  random sequences [26].

We have performed randomized benchmarking using the tetrahedral, octahedral, and icosahedral rotational groups; the results are shown in Fig. 3. As we start by initializing the qubit in the ground state, the sequence fidelity is given by the ground state population after applying the random sequences. The traces follow an exponential decay with increasing  $m$ , as expected. We have also interleaved four gates from the tetrahedral group (see insets for the rotational axes). These rotations are shared by all three rotational groups, allowing for a direct comparison between tetra-, octa-, and icosahedral-based randomized benchmarking. We emphasize that the interleaved gates are physically implemented in exactly the same manner.

From the reference traces, we extract an average error per group of rotations of  $r_{\text{ref,T}} = 9 \times 10^{-4}$ ,  $r_{\text{ref,C}} = 10 \times 10^{-4}$ ,  $r_{\text{ref,I}} = 19 \times 10^{-4}$ . When dividing by  $1\frac{3}{4}$ ,  $1\frac{7}{8}$ , or  $4\frac{4}{15}$ , these numbers consistently point to an average error of  $5 \times 10^{-4}$  per physical gate (single decomposed rotation around the  $X$ ,  $Y$ , or  $Z$  axis). The gate errors are dominated by decoherence [27]. The extracted fidelities for the interleaved gates are tabulated in Fig. 3. The reference error per gate, as well as the errors for the interleaved gates, are consistent with previous measurements [8], where the average physical gate fidelity lies at 0.9994. In

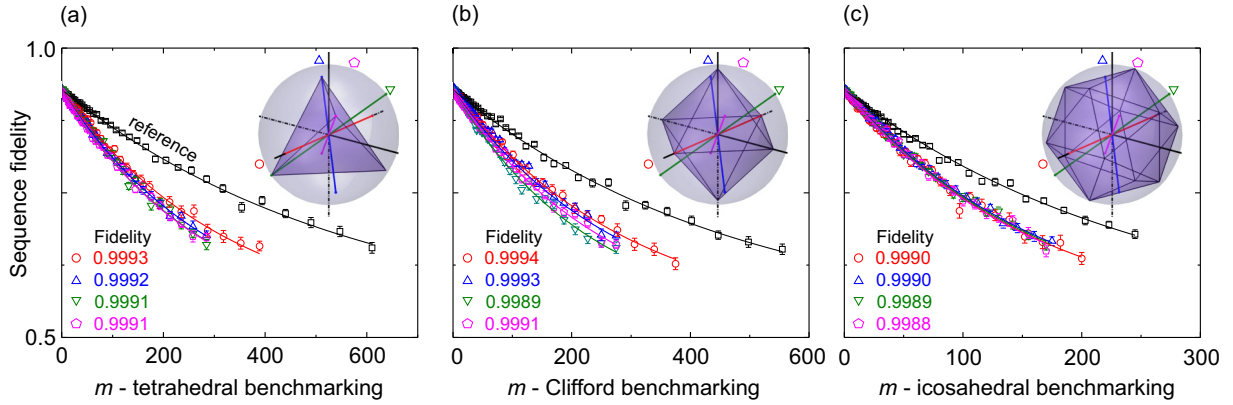


FIG. 3. (Color online) Randomized benchmarking with the (a) tetra-, (b) octa-, and (c) icosahedral rotational groups. The sequence fidelities are plotted as a function of  $m$ , the number of random rotations or sets of random rotation and interleaved gate. For each  $m$ , the fidelity is averaged over  $k = 50$  different, random sequences. From fits to the reference curves (black lines) we extract the average error per group rotation of  $r_{\text{ref},T} = 0.0009$ ,  $r_{\text{ref},C} = 0.0010$ , and  $r_{\text{ref},I} = 0.0019$ , consistent with an average physical gate fidelity of 0.9995. The rotational groups preserve Platonic solids in Bloch space; the respective solids are shown in the insets. The colored lower curves show the data when interleaving four tetrahedral rotations which are shared among all three groups; the rotational axes are shown in the insets; the composed gates are  $X_\pi$  ( $\circ$ ),  $X_{\pi/2} Y_{\pi/2}$  ( $\Delta$ ),  $X_{-\pi/2} Y_{\pi/2}$  ( $\nabla$ ), and  $Y_{\pi/2} X_{\pi/2}$  ( $\diamond$ ). Here,  $X_{\pi/2} Y_{\pi/2}$  denotes the unitary  $R_Y(\pi/2)R_X(\pi/2) = \exp(-i\pi\sigma_Y/4)\exp(-i\pi\sigma_X/4)$ . The gate fidelities are tabulated in the figures, extracted from fits to the data (solid lines). Error bars on the data indicate the standard deviation of the mean. The standard deviations of gate fidelities are typically  $10^{-4}$ .

addition, the mean difference in error of the interleaved gates is below  $2 \times 10^{-4}$  [29], verifying that any of the groups can be used for randomized benchmarking.

With icosahedral randomized benchmarking shown to be a viable method for determining gate fidelity, we can now benchmark gates outside of the Clifford group, as shown in Fig. 4. We chose three composite gates, which are implemented using three, six, or eight physical gates. The rotational axes are highlighted in the inset. The fidelities of these gates are

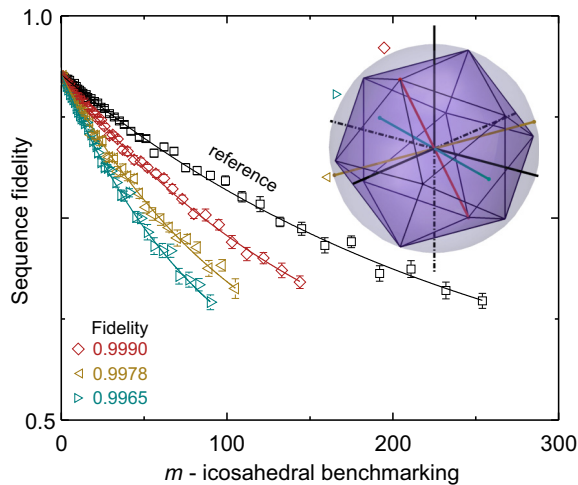


FIG. 4. (Color online) Icosahedral-based randomized benchmarking. We have interleaved three non-Clifford gates whose axes are shown in the inset, the gates rotate around a face center, vertex or edge midpoint of the icosahedron (superimposed). The gates are composed of three, six, and eight elements. Their compositions are:  $Y_\phi X_{2\pi/5} Y_{-\phi}$  ( $\diamond$ ),  $X_\phi Z_{-2\pi/5} Y X_{2\phi} Z_{2\pi/5} X_{-\phi}$  ( $\triangleleft$ ), and  $X_\phi Z_{-2\pi/5} X_{-\phi} X_{-\pi/2} Y_{-\pi/2} X_\phi Z_{2\pi/5} X_{-\phi}$  ( $\triangleright$ ). The gate fidelities are tabulated in the figure. The average error per physical gate which makes up the interleaved gates is  $r = 3 - 4 \cdot 10^{-4}$ .

tabulated in the figure. These complex gates work surprisingly well: We compute the average error per physical decomposition to range between  $3 \times 10^{-4}$  and  $4 \times 10^{-4}$ , assuming that errors are small and uncorrelated. These results demonstrate that even these complex, composite gates can be implemented with high fidelity.

Apart from the first demonstrated implementation of rotational groups beyond the Clifford group, the results on icosahedral benchmarking in Figs. 3 and 4 clearly indicate that physical rotations, other than the widely used Clifford rotations, can be done with a very similar fidelity. This strongly suggests that any arbitrary rotation can be done with high fidelity. Moreover, the gate parameters can be optimized to achieve decoherence-limited performance using the method outlined in Ref. [15], providing an interpolation table for implementing any desired rotation directly, efficiently, and accurately. In addition, icosahedral benchmarking could also be used for evaluating functions of higher order, beyond gate fidelity, as the tetra-, octa-, and icosahedral rotational groups are unitary 2-, 3-, and 5-designs [30,31].

We have shown a quantum version of rolling dice with a superconducting qubit, using gate sets inspired by the Platonic solids. Fundamentally, our work illustrates the potential of using unitaries with a finer distribution for accurate control, and provides a route for the implementation and benchmarking of non-Clifford gates. More generally, our results imply that arbitrary rotations can be done with high accuracy, allowing for complex gates and algorithms to be performed more efficiently in quantum information processing.

R.B. acknowledges G. P. Velders for exhausting demonstrations of rolling dice. This research was funded by the Office of the Director of National Intelligence (ODNI), Intelligence Advanced Research Projects Activity (IARPA), through the Army Research Office Grants No. W911NF-09-1-0375 and No. W911NF-10-1-0334. All statements of fact, opinion, or

conclusions contained herein are those of the authors and should not be construed as representing the official views or policies of IARPA, the ODNI, or the U.S. Government. Devices were made at the UC Santa Barbara Nanofabrication

Facility, a part of the NSF-funded National Nanotechnology Infrastructure Network, and at the NanoStructures Cleanroom Facility.

R.B. and J.K. contributed equally to this work.

- 
- [1] Plato, *Timaeus* (c. 360 BCE), translated by B. Jowett.
- [2] J. Tweet, M. Cook, and S. Williams, *Dungeons and Dragons Player's Handbook* (Wizards of the Coast, Renton, WA, 2000).
- [3] M. B. Hastings, D. Wecker, B. Bauer, and M. Troyer, [arXiv:1403.1539](https://arxiv.org/abs/1403.1539).
- [4] B. P. Lanyon, C. Hempel, D. Nigg, M. Müller, R. Geritsma, F. Zähringer, P. Schindler, J. T. Barreiro, M. Rambach, G. Kirchmair, M. Hennrich, P. Zoller, R. Blatt, and C. F. Roos, *Science* **334**, 57 (2011).
- [5] D. Hanneke, J. P. Home, J. D. Jost, J. M. Amini, D. Leibfried, and D. J. Wineland, *Nat. Phys.* **6**, 13 (2010).
- [6] A. Yu. Kitaev, *Russ. Math. Surv.* **52**, 1191 (1997).
- [7] N. J. Ross and P. Selinger, [arXiv:1403.2975](https://arxiv.org/abs/1403.2975).
- [8] R. Barends, J. Kelly, A. Megrant, A. Veitia, D. Sank, E. Jeffrey, T. C. White, J. Mutus, A. G. Fowler, B. Campbell, Y. Chen, Z. Chen, B. Chiaro, A. Dunsworth, C. Neill, P. O'Malley, P. Roushan, A. Vainsencher, J. Wenner, A. N. Korotkov, A. N. Cleland, and John M. Martinis, *Nature (London)* **508**, 500 (2014).
- [9] C. A. Ryan, M. Laforest, and R. Laflamme, *New J. Phys.* **11**, 013034 (2009).
- [10] T. P. Harty, D. T. C. Allcock, C. J. Ballance, L. Guidoni, H. A. Janacek, N. M. Linke, D. N. Stacey, and D. M. Lucas, [arXiv:1403.1524](https://arxiv.org/abs/1403.1524).
- [11] S. Kimmel, M. P. da Silva, C. A. Ryan, B. R. Johnson, and T. Ohki, *Phys. Rev. X* **4**, 011050 (2014).
- [12] A. D. Córcoles, J. M. Gambetta, J. M. Chow, J. A. Smolin, M. Ware, J. Strand, B. L. T. Plourde, and M. Steffen, *Phys. Rev. A* **87**, 030301 (2013).
- [13] See Supplemental Material at <http://link.aps.org/supplemental/10.1103/PhysRevA.90.030303> for an overview of the used gates and their generators, and details on control.
- [14] R. Barends, J. Kelly, A. Megrant, D. Sank, E. Jeffrey, Y. Chen, Y. Yin, B. Chiaro, J. Mutus, C. Neill, P. O'Malley, P. Roushan, J. Wenner, T. C. White, A. N. Cleland, and J. M. Martinis, *Phys. Rev. Lett.* **111**, 080502 (2013).
- [15] J. Kelly, R. Barends, B. Campbell, Y. Chen, Z. Chen, B. Chiaro, A. Dunsworth, A. G. Fowler, I.-C. Hoi, E. Jeffrey, A. Megrant, J. Mutus, C. Neill, P. J. J. O'Malley, C. Quintana, P. Roushan, D. Sank, A. Vainsencher, J. Wenner, T. C. White, A. N. Cleland, and J. M. Martinis, *Phys. Rev. Lett.* **112**, 240504 (2014).
- [16] E. Lucero, J. Kelly, R. C. Bialczak, M. Lenander, M. Mariantoni, M. Neeley, A. D. O'Connell, D. Sank, H. Wang, M. Weides, J. Wenner, T. Yamamoto, A. N. Cleland, and John M. Martinis, *Phys. Rev. A* **82**, 042339 (2010).
- [17] J. M. Chow, L. DiCarlo, J. M. Gambetta, F. Motzoi, L. Frunzio, S. M. Girvin, and R. J. Schoelkopf, *Phys. Rev. A* **82**, 040305(R) (2010).
- [18] We find that fine-tuning with randomized benchmarking reduces the average error from  $10 \times 10^{-4}$  to  $9 \times 10^{-4}$  per Clifford and  $20 \times 10^{-4}$  to  $19 \times 10^{-4}$  per icosahedral rotation.
- [19] E. Magesan, J. M. Gambetta, and J. Emerson, *Phys. Rev. Lett.* **106**, 180504 (2011).
- [20] D. Gross, K. Audenaert, and J. Eisert, *J. Math. Phys.* **48**, 052104 (2007).
- [21] J. Emerson, R. Alicki, and K. Życzkowski, *J. Opt. B: Quantum Semiclass. Opt.* **7**, S347 (2005).
- [22] C. Dankert, R. Cleve, J. Emerson, and E. Livine, *Phys. Rev. A* **80**, 012304 (2009).
- [23] E. Magesan, J. M. Gambetta, and J. Emerson, *Phys. Rev. A* **85**, 042311 (2012).
- [24] We have verified that the generated gates are a unitary 2-design: A group  $\{U_k\}_{k=1}^K$  is a 2-design if and only if  $\sum_{k,k'=1}^K |\text{Tr}(U_k^\dagger U_{k'})|^4 / K^2 = 2$  [20].
- [25] E. Magesan, J. M. Gambetta, B. R. Johnson, C. A. Ryan, J. M. Chow, S. T. Merkel, M. P. da Silva, G. A. Keefe, M. B. Rothwell, T. A. Ohki, M. B. Ketchen, and M. Steffen, *Phys. Rev. Lett.* **109**, 080505 (2012).
- [26] J. M. Epstein, A. W. Cross, E. Magesan, and J. M. Gambetta, *Phys. Rev. A* **89**, 062321 (2014).
- [27] The qubit had an energy relaxation time of  $T_1 = 28 \mu\text{s}$ , and a Hahn spin echo dephasing time of  $T_2 = 14 \mu\text{s}$ , giving a contribution to gate error of  $4 \times 10^{-4}$  from decoherence [28].
- [28] P. J. J. O'Malley, J. Kelly, and R. Barends *et al.* (unpublished).
- [29] We attribute the small difference between icosahedral and Clifford RB ( $2 \times 10^{-4}$  on average) to imperfections in the frequency detuning control. See Refs. [8] and [15] for details.
- [30] A. Roy and A. J. Scott, *Des. Codes Cryptogr.* **53**, 13 (2009).
- [31] A  $t$ -design is also a  $(t - 1)$ -design.